THE JOURNAL OF BIOLOGICAL CHEMISTRY VOL. 285, NO. 23, pp. 17725–17733, June 4, 2010

Mechanism of Cation Binding to the Glutamate Transporter EAAC1 Probed with Mutation of the Conserved Amino Acid Residue Thr^{101}*[S]

Received for publication, March 9, 2010, and in revised form, April 2, 2010 Published, JBC Papers in Press, April 8, 2010, DOI 10.1074/jbc.M110.121798

Zhen Tao[‡1], **Noa Rosental**[§], **Baruch I. Kanner**[§], **Armanda Gameiro**[‡], **Juddy Mwaura**[‡], **and Christof Grewer**[‡2]

From the [‡]*Department of Chemistry, Binghamton University, Binghamton, New York 13902 and the* [§]*Department of Biochemistry, Hebrew University Hadassah Medical School, Jerusalem 91120, Israel*

The glutamate transporter excitatory amino acid carrier 1 (EAAC1) catalyzes the co-transport of three Na^+ ions, one H^+ ion, and one glutamate molecule into the cell, in exchange for one K^+ ion. Na^+ binding to the glutamate-free form of the transporter generates a high affinity binding site for glutamate and is thus required for transport. Moreover, sodium binding to the transporters induces a basal anion conductance, which is further activated by glutamate. Here, we used the [Na^+] dependence of this conductance as a read-out of Na^+ binding to the substrate-free transporter to study the impact of a highly conserved amino acid residue, Thr^{101}, in transmembrane domain 3. The apparent affinity of substrate-free EAAC1 for Na^+ was dramatically decreased by the T101A but not by the T101S mutation. Interestingly, in further contrast to EAAC1$_{WT}$, in the T101A mutant this [Na^+] dependence was biphasic. This behavior can be explained by assuming that the binding of two Na^+ ions prior to glutamate binding is required to generate a high affinity substrate binding site. In contrast to the dramatic effect of the T101A mutation on Na^+ binding, other properties of the transporter, such as its ability to transport glutamate, were impaired but not eliminated. Our results are consistent with the existence of a cation binding site deeply buried in the membrane and involving interactions with the side chain oxygens of Thr^{101} and Asp^{367}. A theoretical valence screening approach confirms that the predicted site of cation interaction has the potential to be a novel, so far undetected sodium binding site.

Glutamate transporters belong to SLC1 (solute carrier family 1), which consists of glutamate transporters and neutral amino acid transporters (1). One of the major functions of glutamate transporters is to remove the excitatory neurotransmitter glutamate from the synaptic cleft, after it is released from presynaptic neurons, to prevent its concentration from reaching neurotoxic levels (2). Mammalian glutamate transporters consist of five members, excitatory amino acid transporter 1 (EAAT1 or GLAST),[3] EAAT2 (GLT-1), EAAT3 (EAAC1 or excitatory amino acid carrier 1), EAAT4, and EAAT5 (3–7). According to the stoichiometry of these transporters, which co-transport three Na^+ ions and one proton with one glutamate into the cell and counter-transport one K^+ out of the cell (8, 9), transport of glutamate is electrogenic (5, 10, 11), namely, two positive charges are moved into the cell during each transport cycle. In addition to this stoichiometric, or coupled current, glutamate transporters also catalyze a sodium-dependent anion conductance, which is further activated by the substrates of the transporter (4). This anion conductance is specific for hydrophobic anions and is uncoupled from substrate transport itself, a process unaffected by the absence of chloride from both sides of the membrane (12). Glutamate transport is a sequential process where the co-transport of glutamate with three Na^+ and a proton is followed by the counter-transport of K^+ to reset the empty transporter in the outward-facing conformation (13–15) (see Fig. 1*A*). It is thought that the anion conductance is associated with specific states in the transport cycle, in particular those that are populated during the Na^+/glutamate half-cycle (16–19). Bulky glutamate analogues, such as D,L-threo-β-benzoylaspartate (TBOA), can bind to the transporter but are too large to be transported and therefore "lock" the transporter in an outward-facing conformation. These analogues are not only competitive inhibitors of the two types of substrate-induced current but also inhibit the basal sodium-dependent anion conductance (20, 21).

The identification of cation binding sites is a key requirement for our understanding of the coupling of substrate transport to Na^+ transport in Na^+-driven, secondary active transporters. Recently, a crystal structure of GltPh (aspartate transporter from *Pyrococcus horikoshii*) in complex with two Tl^+ ions was published (22). Functional studies indicate that, like in the mammalian counterparts, transport of one aspartate molecule by GltPh is driven by co-transport of at least two Na^+ ions (23). Although substrate transport could not be measured in the presence of Tl^+, it was proposed that the two Tl^+ ions bind to sites (termed Tl1 and Tl2 sites) that also bind Na^+ (22). This proposal was supported by the fact that mutation of one of the amino acids coordinating Tl1, Asp^{405}, to asparagine altered the

* This work was supported, in whole or in part, by National Institutes of Health Grants 2R01NS049335-06A1 (to C. G.) and NS 16708 (to B. I. K.). This work was also supported by Binational Science Foundation Grant 2007051 (to C. G. and B. I. K.) and American Heart Association Grant 0525485B (to Z. T.).

[S] The on-line version of this article (available at http://www.jbc.org) contains supplemental Figs. S1 and S2.

[1] Present address: Membrane Transport Biophysics Unit, NINDS, National Institutes of Health, Bethesda, MD 20892-3701.

[2] To whom correspondence should be addressed: Dept. of Chemistry, Binghamton University, 4400 Vestal Parkway East, Binghamton, NY 13902. Tel.: 607-777-3250; Fax: 607-777-4478; E-mail: cgrewer@binghamton.edu.

[3] The abbreviations used are: EAAT, excitatory amino acid transporter; EAAC, excitatory amino acid carrier; TBOA, D,L-threo-β-benzoylaspartate; WT, wild type; MES, 4-morpholineethanesulfonic acid.

experimentally observed Na^+:Asp coupling ratio of 2:1 to a coupling ratio of 1.5:1 (22). This change in coupling ratio caused by the D405N mutation, which is equivalent to the EAAC1 D454N mutation (24), was interpreted as partial coupling of the Na^+ bound to the Tl1 site to aspartate binding (22). Binding of Na^+ to the Tl1 and Tl2 sites is also supported by computational studies (25, 26) and a valence scanning analysis (27). Moreover, a recent study on EAAC1 indicates that the conserved aspartate from the Tl1 site participates in an overlapping sodium and potassium binding site (28).

Functional studies have identified a highly conserved aspartate residue in TMD7, Asp^{367} (29), which upon mutagenesis to asparagine led to a >16-fold reduction in sodium affinity (24). In contrast to this dramatic effect of the D367N mutation, the D454N exchange did not reduce the Na^+ affinity of EAAC1 (24), whereas both mutations potently reduced the affinity of EAAC1 for Tl^+ (30). Based on these data, it was hypothesized that an additional Na^+ binding site exists that is buried deeply in the membrane, which involves the side chain of Asp^{367} (24). Analyses of the crystal structure of GltPh and homology models of EAAC1 built from this structure reveal that another conserved amino acid side chain, Thr^{101} of EAAC1, protrudes into a hydrophilic cavity also occupied by the Asp^{367} side chain. Therefore, it is possible that the Thr^{101} hydroxy oxygen also contributes to coordinating a cation.

In this work, we have tested this hypothesis by studying the effects of mutations to residue Thr^{101} in EAAC1. Thr^{101} is highly conserved among all SLC1 family members (see Fig. 1*B*). The apparent affinity of the glutamate-free/bound form of the transporter for Na^+ ions was determined, showing a drastic increase in the K_m of the empty transporter for Na^+ upon mutating Thr^{101} to alanine. Furthermore, the data showed that two Na^+ ions bind to the glutamate-free, empty form of the T101A transporter. These results suggest the existence of an additional cation binding site not observed in the GltPh crystal structure, which is in agreement with calculations from a valence mapping approach.

MATERIALS AND METHODS

Molecular Biology and Transient Expression—Wild type EAAC1 cloned from rat retina was subcloned into pBK-CMV (Stratagene) as described previously (20) and was used for site-directed mutagenesis according to the QuikChange protocol (Stratagene, La Jolla, CA) as described by the supplier. The primers for mutation experiments were obtained from the DNA core lab of the Department of Biochemistry at the University of Miami School of Medicine. The complete coding sequences of mutated EAAC1 clones were subsequently sequenced. Wild type and mutant EAAC1 constructs were used for transient transfection of subconfluent human embryonic kidney cell (HEK293T/17, ATCC number CRL 11268) cultures using FuGENE 6 transfection reagent (Roche Applied Science) according to the supplied protocol. Electrophysiological recordings were performed between days 1 and 3 post-transfection.

For uptake experiments, the C-terminal histidine-tagged version of rabbit EAAC1 (WT) in the vector pBluescript was used as a parent vector for site-directed mutagenesis (31, 32). This was followed by subcloning of the mutation into the WT construct residing in the oocyte expression vector pOG1 (49), using the unique restriction enzymes MluI and PflMI. The subcloned DNA fragment was sequenced between these unique restriction sites.

Uptake Assays—HeLa cells were cultured (33), infected with the recombinant vaccinia/T7 virus vTF$_{7-3}$ (34), and transfected with the plasmid DNA harboring the WT or Thr^{101} mutants or with the plasmid vector alone (33). Transport of L-[^{3}H]aspartate was done as described (32). L-[^{3}H]Aspartate was used rather than L-[^{3}H]glutamate, because of the low background values obtained in HeLa cells transfected with the vector alone. Briefly, HeLa cells were plated on 24-well plates and washed with transport medium containing 150 mM NaCl, and 5 mM potassium phosphate, pH 7.4. Each well was then incubated with 200 μl of transport medium supplemented with 0.4 μCi of L-[^{3}H]aspartate and incubated for 3 min (because transport as a function of time is linear up to 3 min), followed by washing, solubilization of the cells with SDS, and scintillation counting. To determine the rate dependence of transport on the sodium ion concentration, NaCl was replaced by choline chloride to a total concentration of 150 mM, during both washing and transport.

Electrophysiology—Glutamate-induced EAAC1 currents were recorded with an Adams & List EPC7 amplifier under voltage clamp conditions in the whole cell current recording configuration (20). The typical resistance of the recording electrode was 2–3 MΩ; the series resistance was 5–8 MΩ. Because the glutamate-induced currents were small (typically <500 pA), series resistance (R_S) compensation had a negligible effect on the magnitude of the observed currents (<4% error). Therefore, R_S was not compensated. If not otherwise noted, the extracellular solution contained 140 mM NaCl or 140 mM NaMES, 2 mM $CaCl_2$, 2 mM $MgCl_2$, and 30 mM HEPES (pH 7.4/NaOH). Two different pipette solutions were used depending on whether mainly the noncoupled anion current (with thiocyanate) or the coupled transport current (with MES^-) was investigated (18). These solutions contained 140 mM KSCN or KMES, 2 mM $MgCl_2$, 10 mM EGTA, and 10 mM HEPES (pH 7.4/KOH). Thiocyanate was used because it enhances glutamate transporter-associated currents and allows the detection of the EAAC1 anion conducting mode (35).

For the electrophysiological investigation of the Na^+/glutamate homoexchange mode, the pipette solution contained 140 mM NaMES or NaSCN, 2 mM $MgCl_2$, 10 mM EGTA, 10 mM glutamate, and 10 mM HEPES (pH 7.4/NaOH). In this transport mode, a constant intracellular concentration of 140 mM Na^+ is used, and concentrations of glutamate are used on the intra- and extracellular sides that saturate their respective binding site. The apparent affinity of EAAC1 for cytoplasmic glutamate is 280 μM (19). Therefore, we used 10 mM cytoplasmic glutamate to ensure saturation of the intracellular binding site. In contrast, the apparent affinity for extracellular glutamate is ~6 μM (20), and 100–200 μM extracellular glutamate is sufficient for saturation of this binding site. Initially, glutamate was omitted from the extracellular solution. Under these conditions, the high intracellular Na^+ and glutamate concentrations will drive the majority of glutamate binding sites to face the extracellular side. Subsequently, application of extracellular glutamate

resulted in a redistribution of these binding sites to reach a new steady state. According to the nature of the exchange mode, it is not associated with steady-state transport current. However, transient transport currents were observed when glutamate was applied to the extracellular side of the membrane, because of the electrogenic redistribution of Na^+ and glutamate binding sites within the membrane (18). When permeating anions, such as SCN^-, are present, establishment of homoexchange conditions leads to the permanent activation of an anion current (18, 36). This permanent anion current was used here as a tool to study the behavior of mutant transporters in the homoexchange mode. If not stated otherwise, the pH of the solutions was 7.4.

The currents were low pass filtered at 1–10 kHz (Krohn-Hite 3200) and digitized with a digitizer board (Axon, Digidata 1200) at a sampling rate of 10–50 kHz, which was controlled by software (Axon PClamp). All of the experiments were performed at room temperature.

Laser Pulse Photolysis and Rapid Solution Exchange—Rapid solution exchange was performed as described previously (20). Briefly, substrates were applied to the EAAC1-expressing cell by means of a quartz tube (opening diameter, 350 μm) positioned at a distance of ~0.5 mm to the cell. The linear flow rate of the solutions emerging from the opening of the tube was ~5–10 cm/s, resulting in typical rise times of the whole cell current of 30–50 ms (10–90%). Laser pulse photolysis experiments were performed according to previous studies (37, 38). 4-Methoxy-7-nitroindolinyl-caged glutamate (39) (Tocris) in concentrations of 1–4 mM or free glutamate were applied to the cells, and photolysis of the caged glutamate was initiated with a light flash (351 nm, diode-pumped Nd:YAG-laser, frequency-tripled; Continuum). The light was coupled into a quartz fiber (diameter, 365 μm) that was positioned at a distance of 300 μm from the cell. The laser energy was adjusted with neutral density filters (Andover Corp.). With maximum light intensities of 500–600 mJ/cm^2, saturating glutamate concentrations could be released, which was tested by comparison of the steady-state current with that generated by rapid perfusion of the same cell with a glutamate concentration that saturated the transporter under study. In rare cases HEK293 cells respond to the laser flash with small transient current responses (<10 pA) in the absence of caged compound. Such cells were discarded.

Valence Mapping—To test for potential cation binding sites, we performed valence mapping according to the procedure developed by Page and Di Cera (40). We used the Vale program for screening the GltPh crystal structure for coordinates with appropriate valences (41). Valences between 0.8 and 1.2 were then mapped onto the GltPh structure file (Protein Data Bank entry 1XFH) (42). After candidates were found, the theoretical valence for the cation binding site was calculated using the following equation.

$$V_{\text{Cation}+} = \sum(R_i/R_0)^{-N} \qquad \text{(Eq. 1)}$$

Here, R_i is the distance between the cation and a neighboring oxygen atom, and R_0 is the value of R_i for $\nu_{\text{Cation}+} = 1$. R_0 and N are empirical values for cation-oxygen pairs, which depend on the identity of the bound cation. A suitable monovalent cation binding site is expected to have a valence of close to 1 with a R_0 of 1.622 Å and $n = 4.29$ (Na^+-O pair) or with $R_0 = 2.276$ Å and $n = 9.1$ (K^+-O pair) (40). According to this procedure, the valence of the proposed cation$^+$ binding site was calculated as 1.17 for K^+ and 0.59 for Na^+.

Data Analysis—Nonlinear regression fits of experimental data were performed with Origin (OriginLab, Northampton, MA) or Clampfit (pClamp8 software; Axon Instruments, Foster City, CA). Pre-steady-state currents were fitted with sums of two or three exponential terms. Dose-response relationships of currents were fitted with a Michaelis-Menten-like equation, yielding K_m and I_{max}. The errors in kinetic parameters are given as standard deviations and were determined from at least four independent experiments from at least three different cells.

RESULTS

The Apparent Affinity of the Transporter for Na^+ Ion(s) Is Decreased by the T101A Mutation—The apparent affinity of the glutamate-free form of $EAAC1_{T101A}$ was detected by using the [Na^+]-induced anion current as an assay, as detailed in Ref. 24. Anion currents induced by application of different [Na^+] to $EAAC1_{T101A}$-expressing HEK293 cells were measured with 140 mM NaSCN and 10 mM glutamate in the pipette solution (V_m = 0 mV) to ensure that the cation binding sites are exposed to the extracellular side (in the absence of external glutamate). Typical current recordings are shown in Fig. 1*C*. As in $EAAC1_{WT}$, the Na^+-induced anion current in $EAAC1_{T101A}$ was strongly dependent on the sodium concentration, as shown in Fig. 1*C*. However, whereas the anion current induced by Na^+ was always inwardly directed in $EAAC1_{WT}$ (because of SCN^- outflow), apparent outward current was observed in $EAAC1_{T101A}$ at [Na^+] below 200 mM, which reverted to the expected inward current at higher [Na^+] (Fig. 1, *C* and *D*) in a biphasic nature. Outward current was never observed in the absence of the permeant anion SCN^- (Fig. 1*D*, *open square*) and in control cells (Fig. 1*C*, *left panel*, *red trace*), suggesting that this current component is anion current specifically carried by the mutant transporter.

As described previously (24), the [Na^+] dependence of the $EAAC1_{WT}$ anion current was well described with a simple Michaelis-Menten-type equation. In contrast, the $EAAC1_{T101A}$ data required a sum of two Michaelis-Menten terms for a satisfactory fit of the biphasic curve, suggesting the existence of two separate Na^+ binding processes. The apparent dissociation constant of the low affinity Na^+ association process could not be determined precisely, because of our inability to apply [Na^+] higher than 300 mM, but it can be estimated as $K_{Na} > 500$ mM (Fig. 1, *D* and *E*). The K_{Na} for the higher affinity step was estimated to 110 mM from a fit of a sum of two Michaelis-Menten equations to the data. For wild type EAAC1, the K_{Na} was ~90 mM (Fig. 1, *D* and *E*), indicating that one Na^+ binds to $EAAC1_{T101A}$ with similar affinity as to the wild type transporter, whereas binding of a second Na^+ ion is severely impaired in its affinity.

In contrast to T101A, the more conservative T101S mutation had little effect on the [Na^+] dependence of the leak anion current (K_{Na} = 105 ± 10 mM), although the amplitude of the leak current was reduced compared with $EAAC1_{WT}$ (Fig. 1, *D*

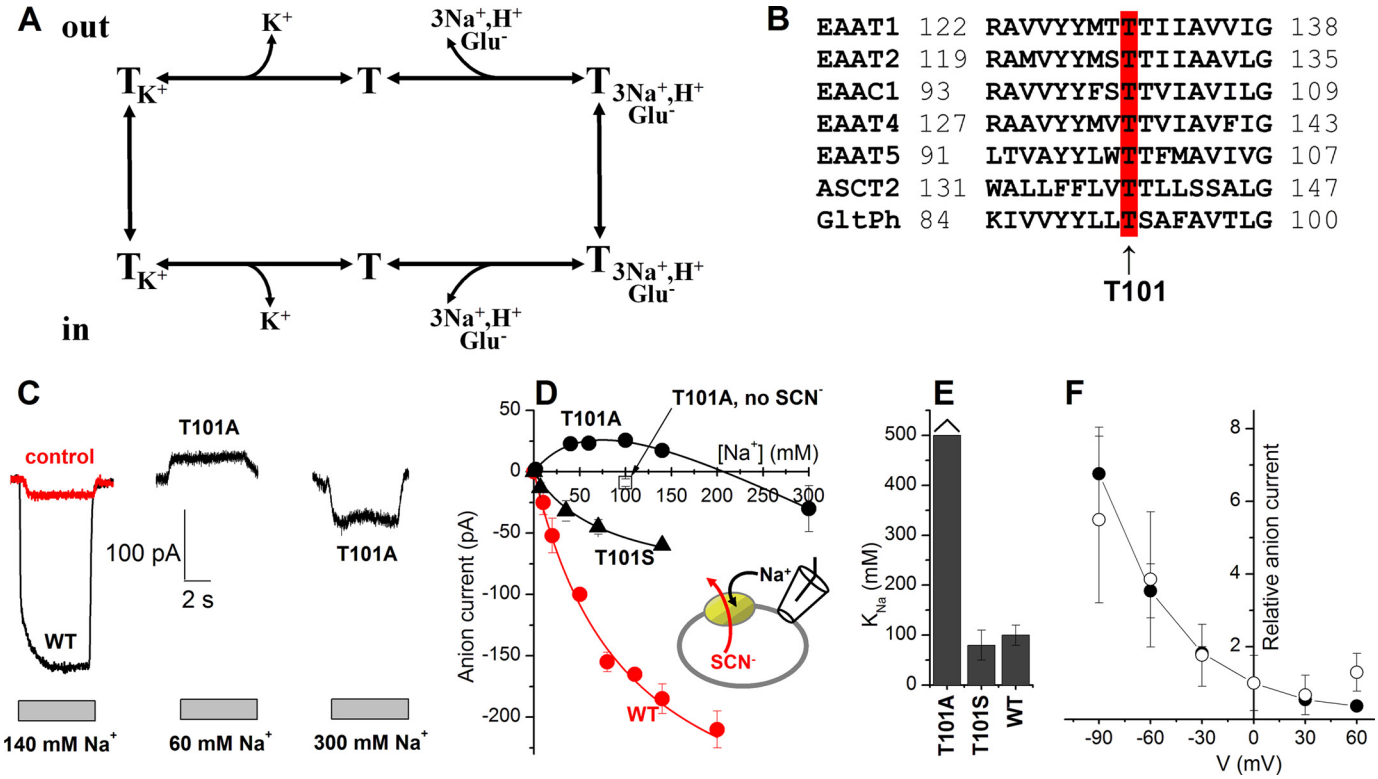

FIGURE 1. **Mutation of Thr[101] to alanine interferes with the ability of Na^+ to induce anion current.** *A*, illustration of the transport cycle. *B*, multiple sequence alignment of EAATs and GltPh shows that Thr[101] (*red*, *arrow*) is conserved within the glutamate transporter family. *C*, typical leak anion currents induced by Na^+ application to $EAAC1_{WT}$ in the absence of external substrate (*left panel*, *black*), nontransfected control cells (*left panel*, *red*), and $EAAC1_{T101A}$ (*middle* and *right panels*). The *gray bars* indicate the length of Na^+ application. The extracellular solution contained MES as the anion and Na^+/NMG^+. The intracellular solution contained 140 mM SCN^- and 10 mM glutamate (see *inset* in *C*). *D*, [Na^+] dependence of specific leak anion currents (*red circles*, WT; *black circles*, T101A; *black triangles*, T101S, control responses were subtracted; *open square*, control response in the absence of SCN^-). The *lines* represent fits to the Michaelis-Menten equation (WT, T101S) or a sum of two Michaelis-Menten equations (T101A). *E*, K_{Na}^+ values determined from the fits. *F*, voltage dependence of the 60 mM Na^+-induced apparent outward current (T101A, *open circles*) indicates that it is mediated by inhibition of a tonic inward anion conductance. For comparison, inhibition of the tonic leak anion conductance of $EAAC1_{WT}$ by TBOA as a function of the voltage is shown as the *solid circles*.

and *E*). No apparent outward current was observed in $EAAC1_{T101S}$. The K_{Na} data are summarized in Fig. 1*E*.

The apparent outward current induced by [Na^+] lower than 200 mM in $EAAC1_{T101A}$ (Fig. 1, *C* and *D*) is most likely due to the inhibition of a tonic outflow of SCN^- in the empty transporter by binding of one Na^+ ion. Consistent with this hypothesis, the voltage dependence of 100 mM [Na^+]-induced current in $EAAC1_{T101A}$ showed an enhanced effect at more negative membrane potential but the absence of reversal at positive potentials (Fig. 1*F*). At −90 mV, the apparent outward current was 57 ± 24 pA, whereas at +30 mV the current was only 7 ± 5 pA. This result was expected if this current is caused by the inhibition of outflow of SCN^-, as shown by the similar *I-V* relationship of inhibition of the Na^+-induced anion current (Fig. 1*F*) by TBOA, which is a nontransportable inhibitor (43). TBOA and other competitive blockers are known to block the anion conductance of glutamate transporters (16, 20).

It is known that the binding of sodium ions or conformational changes associated with it can induce charge movement in EAAC1 (11, 18). This charge movement can be blocked in the presence of TBOA. At 140 mM Na^+, the Na^+ binding site should be approximately half-saturated at 0 mV (44). Thus, voltage-induced charge movements should be large at this [Na^+]. Consistent with this hypothesis, large TBOA-sensitive charge movements were observed in response to voltage jumps applied to HEK293 cells expressing EAAC1 wild type transporters (Fig. 2*A*). To exclude a change in membrane capacitance during the voltage jump protocol, the voltage jump-induced transient currents measured before and after TBOA application were subtracted from each other, showing no difference (Fig. 2, *B* and *D*). Transient currents were also absent in control, nontransfected cells. In contrast to $EAAC1_{WT}$, little TBOA-sensitive charge movement was detected in $EAAC1_{T101A}$-expressing cells (Fig. 2*C*; little charge movement can be induced even by a driving force as high as −150 mV). This result is consistent with a low saturation of at least one Na^+ binding site, because the Na^+ concentration (140 mM) is far below the apparent K_{Na} for Na^+ binding. This indicates that the affinity of the glutamate-free form of $EAAC1_{T101A}$ for Na^+ is very low, consistent with the result from the [Na^+] jump experiment described above.

We next tested the effect of [Na^+] on substrate uptake, as shown in Fig. 3. In agreement with the effect of the T101A mutation on Na^+ affinity predicted by the above experiments, $EAAC1_{T101A}$ required significantly higher [Na^+] to activate L-aspartate uptake than the wild type transporter (Fig. 3), whereas the T101S mutation had little effect on [Na^+] dependence of uptake. The positive cooperativity observed, with n_H values of 2.42 ± 0.55, 1.78 ± 0.15, and 2.13 ± 0.42 for T101A,

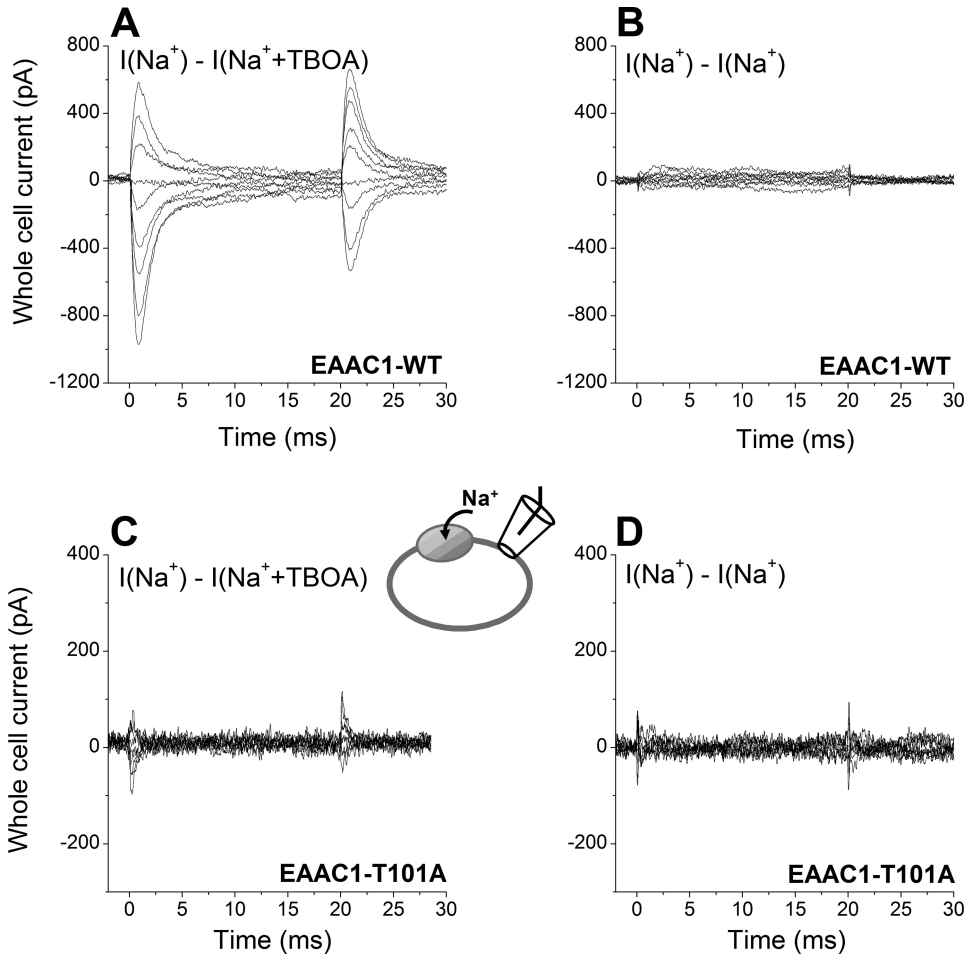

FIGURE 2. **Na^+-dependent transient currents in response to voltage jumps are abolished by the T101A mutation.** *A*, EAAC1-specific transient currents measured in $EAAC1_{WT}$ in response to voltage jumps at time 0 from 0 mV to voltages ranging from +60 to −100 mV in 20-mV increments. $I(Na^+) - I(Na^+ + TBOA)$ represents the current in 140 mM extracellular Na^+, from which the current in the presence of 140 mM Na^+ + 0.1 mM TBOA (a saturating concentration) was subtracted. TBOA blocks only the EAAC1-specific component of the current response. The extracellular solution contained 140 mM NaMES. The intracellular solution contained 140 mM NaMES and 10 mM glutamate. *B*, to test for changes in membrane capacitance during the voltage jump protocol, currents were measured before and after TBOA application. Upon subtraction from each other ($I(Na^+) - I(Na^+)$), these currents show no difference. *C* and *D*, similar experiments as in *A* and *B* for $EAAC1_{T101A}$.

T101S, and WT, respectively ($n = 3$), is consistent with the requirement of three sodium ions/substrate molecule transported (8, 9).

Affinities of the Glutamate-bound Transporter for Glutamate and Na^+—In addition to the two Na^+ ions binding to the empty transporter, it was proposed that a third Na^+ ion associates with the glutamate-bound form of EAAC1 (18). The apparent affinity of EAAC1 for this third sodium can be determined when saturating glutamate concentration is used. These conditions lead to a shift in the Na^+ binding equilibrium of the empty transporter to the fully Na^+-bound form, thus eliminating the effects of these initial Na^+ binding steps on the $[Na^+]$ dependence of the current. To determine which glutamate concentration is saturating, we first measured the apparent dissociation constant (K_m) of the transporter for glutamate as a function of $[Na^+]$, as shown in Fig. 4. Whole cell anion currents were recorded in the exchange mode with 140 mM NaSCN and 10 mM glutamate in the pipette solution, $V_m = 0$ mV. Fig. 4*A* shows a typical current induced by application of 5 mM glutamate to a $EAAC1_{T101A}$-expressing HEK293T cell. The current-[glutamate] relationships of $EAAC1_{T101A}$ at 20, 140, and 300 mM $[Na^+]$ are shown in Fig. 4*B*. At 140 mM $[Na^+]$, the K_m of $EAAC1_{T101A}$ for glutamate was 1.2 ± 0.1 mM ($n = 3$). This value is ~160-fold higher than that of wild type EAAC1. When $[Na^+]$ was raised, the K_m of $EAAC1_{T101A}$ for glutamate decreased (Fig. 4, *B* and *C*), as expected if Na^+ binding to the empty transporter is required for the generation of a high affinity glutamate binding site. The K_m-$[Na^+]$ relationship was linear on a log scale, as shown in Fig. 4*C*. This is consistent with the result obtained previously with $EAAC1_{WT}$ and $EAAC1_{D367N}$. According to this K_m-$[Na^+]$ relationship, 5.3 M $[Na^+]$ would be needed in order for the K_m of $EAAC1_{T101A}$ for the substrate to become similar to that of wild type transporter at 140 mM $[Na^+]$ (K_m = 7.2 μM), consistent with the idea that a lack of saturation of the initial Na^+ binding site(s) reduces the apparent affinity for the substrate.

As shown in Fig. 5 (*closed squares*), a saturating glutamate concentration induced anion currents in $EAAC1_{T101A}$ that were highly $[Na^+]$-dependent. The data could be represented by the Hill equation with a Hill co-efficient of $n = 1.7$ and an apparent dissociation constant of $K_{Na} = 61 \pm 12$ mM. For $EAAC1_{WT}$, the dissociation constant of Na^+ to glutamate-bound form transporter was 18.0 ± 2.0 mM (Fig. 5, *triangles*), with a Hill co-efficient of 1.4. Therefore, the K_{Na} of $EAAC1_{T101A}$ was approximately three times higher than that of wild type EAAC1, indicating that the effect of the mutation on Na^+ binding to the empty transporter is more dramatic than that on Na^+ binding to glutamate-bound EAAC1.

The T101A Mutation Slows but Does Not Eliminate Steady-state Glutamate Transport—As shown in Fig. 6 (*A* and *C*), application of 10 mM glutamate to $EAAC1_{T101A}$-expressing HEK293T cells (the pipette solution contained KMES, $V_{hold} = 0$ mV) generated a small, but significant transport current (−15 ± 2 pA, which is 3.5-fold larger than the current in non-transfected cells). Because there was no permeable anion present, only the coupled transport component of the current should be observed under these conditions. Increasing the electrical driving force enhanced the transport current (Fig. 6*B*, *closed squares*). This behavior was very similar to that of wild type EAAC1 (Fig. 6*B*, *open circles*), although transport currents

in $EAAC1_{WT}$ were on average 6-fold larger than those observed in $EAAC1_{T101A}$. This result indicates that steady-state substrate transport is inhibited but not eliminated by the T101A mutation.

To determine which step of the transport cycle is affected by the mutation, we measured steady-state anion current in response to glutamate application. It was previously shown that transporters with mutations impairing the K^+-dependent relocation but not Na^+-dependent glutamate exchange lack steady-state anion current in the presence of intracellular K^+ but catalyze anion flux in the presence of intracellular Na^+ and glutamate (exchange conditions) (45). $EAAC1_{T101A}$ shows a similar phenotype (Fig. 6*C*), consistent with the possibility that K^+-dependent relocation is slowed but not abolished in the mutant transporter.

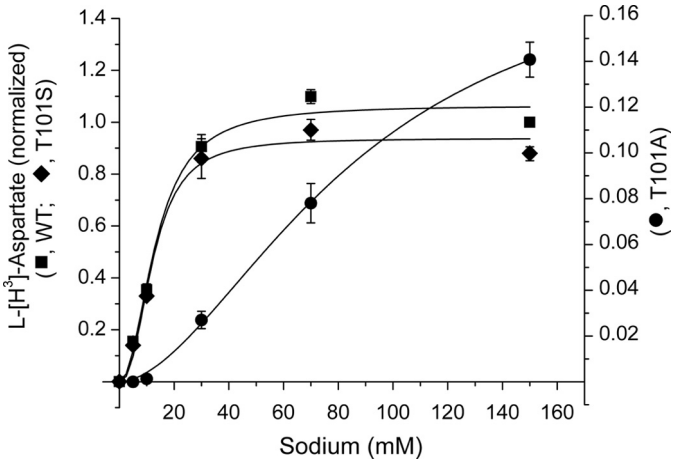

FIGURE 3. **Sodium concentration dependence of L-[^{3}H]aspartate transport.** The rates of transport of $EAAC1_{WT}$ (*squares*), $EAAC1_{T101S}$ (*diamonds*), and $EAAC1_{T101A}$ (*circles*), expressed in HeLa cells, on the sodium concentration were measured as described under "Experimental Procedures" after subtraction of the values for HeLa cells transfected with the vector alone. All of the values, including those of the T101A mutant (*right ordinate*; note the different scale caused by the lower uptake of the mutant), are normalized to those of $EAAC1_{WT}$ at 150 mM NaCl and are the averages ± S.E. of three different experiments each done in quadruplicate.

An alternative explanation for the low transport activity would be that the expression level of $EAAC1_{T101A}$ in the cell membrane is much lower than that of wild type EAAC1. To test this possibility, the expression levels of wild type and T101A mutant transporters were compared by isolating the membrane fraction using cell surface biotinylation labeling, followed by Western blotting. The result shows that the expression levels of the wild type and mutant transporters are similar (see supplemental Fig. S1). Thus, reduced cell surface expression is not responsible for the low transport activity in $EAAC1_{T101A}$. In contrast to T101A, the T101S mutation had little effect on transport current, voltage dependence of transport, and anion current in the exchange and forward transport modes (Fig. 6, *B* and *C*).

The T101A Mutation Slows Glutamate Translocation—To determine the rate of glutamate translocation, we analyzed pre-steady-state currents in response to glutamate concentration jumps. As shown in Fig. 7*A*, in exchange transport mode (140 mM NaMES and 10 mM glutamate in pipette solution, without permeable anion SCN^-) glutamate released from 4 mM 4-methoxy-7-nitroindolinyl-glutamate by laser pulse photolysis induced a transient inward current. After reaching a peak value of approximately −70 pA, the current decayed to a steady state of 0 pA, because there is no net glutamate transport in the exchange mode. This transient current was similar to that of $EAAC1_{WT}$ (Fig. 7*B*) in that it decayed with two exponential components, reflecting separate steps in the glutamate translocation process. However, in comparison with wild type EAAC1, the decay steps for $EAAC1_{T101A}$ were slower. In particular the rate-limiting, slowly decaying phase was associated with an average time constant of 26 ± 4 ms, which was approximately three times larger than that of wild type EAAC1 (8.7 ± 1.7 ms). These results show a significant although not dramatic reduction of the exchange rate by the T101A mutation.

DISCUSSION

We studied the effects of mutation of a conserved amino acid residue, Thr^{101}, which we hypothesize to contribute its side

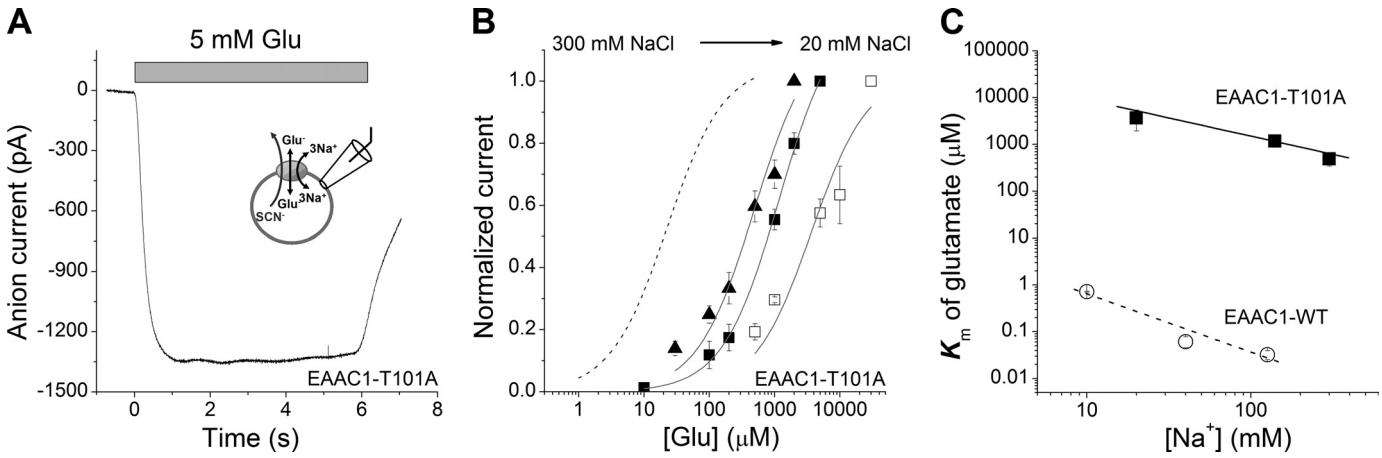

FIGURE 4. **Increased occupancy of the Na^+ binding site(s) increases the glutamate affinity of EAAC1.** *A*, typical anion current in response to 5 mM glutamate applied to $EAAC1_{T101A}$ in the exchange mode (see *inset*). *B*, normalized glutamate dose-response curves as a function of extracellular [Na^+] (300 mM (▲), 140 mM (■), and 20 mM (□)) in exchange mode. The *dotted line* represents the wild type curve at 140 mM Na^+. The currents were normalized to the response at 30 mM glutamate (20 mM Na^+), 5 mM glutamate (140 mM Na^+), and 2 mM glutamate (300 mM Na^+). The extracellular solution contained MES as the anion and the indicated Na^+ concentration supplemented with NMG^+ to 300 mM. The composition of the internal solution was 140 mM NaSCN and 10 mM glutamate, and the transmembrane potential was 0 mV. *C*, [Na^+] dependence of the K_m of $EAAC1_{WT}$ (*open circles*) and $EAAC1_{T101A}$ (*closed squares*) for glutamate.

chain oxygen atom to the coordination of a cation bound to glutamate transporters. The results obtained in this work support this hypothesis for the following reason: the T101A mutation had a dramatic effect on the Na^+ apparent affinity of the empty transporter, determined in the absence of glutamate, reducing this apparent affinity ~10-fold. This result is in agreement with a previous report on mutation of the conserved Asp^{367} residue (24), whose side chain is close in space to the Thr^{101} side chain, as predicted by the GltPh crystal structure. The D367N mutation also led to a large reduction of the Na^+ apparent affinity of EAAC1 (24).

In addition, the T101A mutation reduced Na^+-dependent charge movements in response to voltage jumps, as expected if the Na^+ binding site is little occupied at 140 mM extracellular Na^+. Like in $EAAC1_{D367N}$, the effect of the mutation is more pronounced for Na^+ binding to the empty transporter than to the glutamate-bound EAAC1. In the latter case, the apparent affinity was only reduced by a factor of ~3 (Fig. 5). This result is consistent with the idea that the cation binding site equivalent to the Tl2 site of GltPh, which requires bound substrate to be occupied, is located in proximity to the substrate binding site, but several Angstroms removed from the location of the Thr^{101} mutation. Thus, the effect on Na^+ association with the Tl2 site appears to be indirect, as proposed for $EAAC1_{D367N}$ (24).

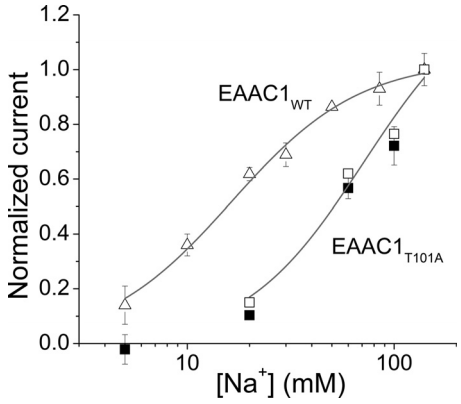

FIGURE 5. **Determination of the affinity of the glutamate-bound transporter for Na^+.** Anion currents were determined as a function of [Na^+] at a close to saturating concentration of 30 mM glutamate ($EAAC1_{WT}$, *triangles*; $EAAC1_{T101A}$, *closed squares*; no currents were induced when the glutamate was substituted by 30 mM MES^-). The *open squares* represent I_{max} values calculated by extrapolation according to the K_m values for glutamate at each [Na^+] shown in Fig. 4*C*. The *solid lines* represent fits to the Hill equation (fit parameters in main text). All of the experiments were performed in the exchange mode and at 0 mV transmembrane potential. The currents were normalized to the response induced by 140 mM Na^+.

The Binding of Two Na^+ Ions to the Glutamate-free Form of $EAAC1_{T101A}$ Is Required for Anion Conductance Activation—Anion current induced by applying different [Na^+] to $EAAC1_{T101A}$ showed biphasic dose dependence (Fig. 1*D*), a behavior that was not observed in wild type EAAC1 or other mutant transporters studied so far. This biphasic behavior cannot be explained by assuming that only one Na^+ binds to the glutamate-free form of the transporter. However, the data can be very well explained by assuming that two Na^+ ions bind to the transporter in the absence of glutamate, in agreement with a recent proposal based on fluorescence labeling experiments (46). A kinetic model depicting this binding sequence is shown in Fig. 8, and simulations of anion current according to this model are shown in supplemental Fig. S2, suggesting that binding of two Na^+ ions to the glutamate-free transporter is required to form a high affinity substrate binding site. Therefore it is likely that under forward transport conditions the sequence of binding events is as follows: two Na^+ ions associate sequentially with the transporter, followed by binding of the transported substrate (Fig. 8). Once the Na_2-transporter-Glu complex is formed, a third binding site for Na^+ becomes available that must be occupied to allow translocation. This third binding site is possibly analogous to the Tl2 site of GltPh, which is only occupied in the presence of transported substrates but which is not occupied in the presence of nontransportable inhibitors, such as TBOA (22). Why is the biphasic behavior of the [Na^+] dependence of the anion current not observed in $EAAC1_{WT}$? The most likely reason is that Na^+ ions associate with $EAAC1_{WT}$ with much higher affinity than with the T101A mutant transporter, as shown in Fig. 8. In fact, simulations of anion current amplitudes as a function of [Na^+] demonstrate that the experimental results can be reproduced by assuming a 7–14-fold reduction of Na^+ affinity by the T101A mutation (supplemental Fig. S2). However, it should be noted that anion conductance levels are also altered by the T101A mutation (supplemental Fig. S2) and that it cannot be ruled out that the T101A mutation alters the sequence of sodium binding.

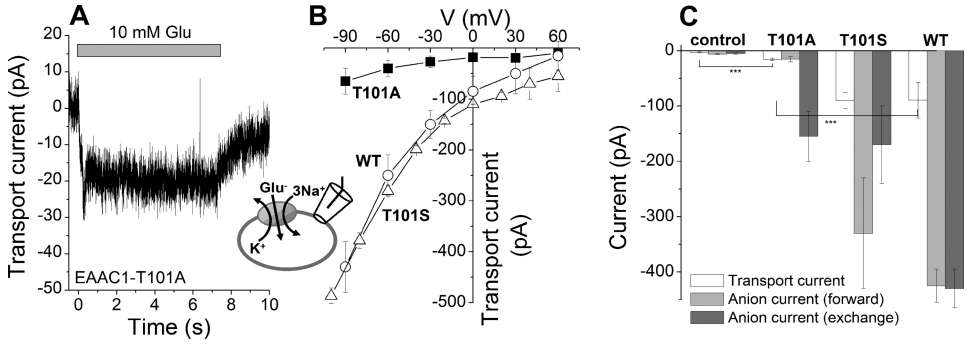

FIGURE 6. **The T101A mutation inhibits steady-state glutamate transport.** *A*, typical transport current induced by 10 mM glutamate application to $EAAC1_{T101A}$ (V_m = 0 mV; the extracellular solution contained MES^- as the anion and 140 mM Na^+, and the intracellular solution contained 140 mM KMES). *B*, transport current-voltage relationships for $EAAC1_{T101A}$ (*solid squares*), $EAAC1_{T101S}$ (*open triangles*), and $EAAC1_{WT}$ (*open circles*). *C*, average transport currents (*white bars*) and anion currents in the forward transport mode (*light gray bars*, 140 mM KSCN internal) and exchange mode (*dark gray bars*, 140 mM NaSCN, 10 mM glutamate internal) at 0 mV transmembrane potential. The control cells were nontransfected. The glutamate concentration was 10 mM.

We propose a sequential binding model deduced from the T101A

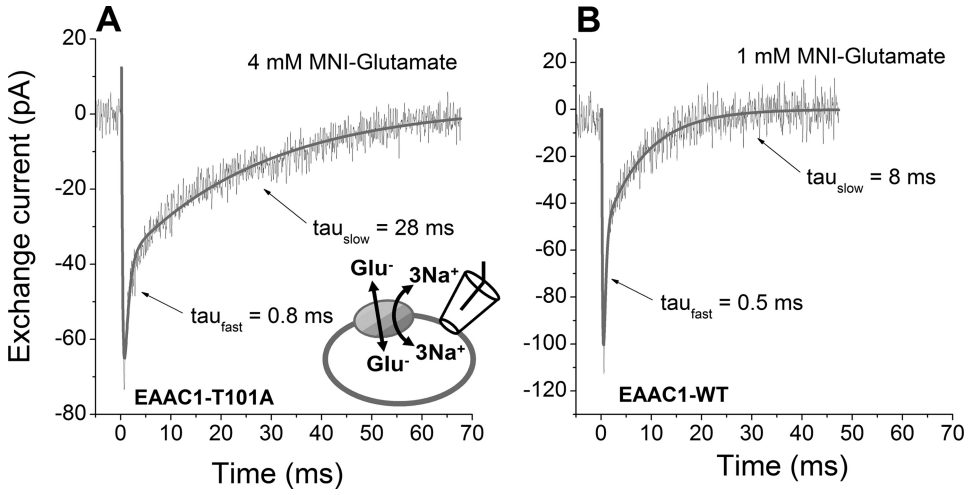

FIGURE 7. **EAAC1$_{T101A}$ is active in exchange mode, but with slowed exchange kinetics.** *A*, typical transport current elicited by a glutamate concentration jump at time $t = 0$, generated by laser flash photolysis of 4 mM 4-methoxy-7-nitroindolinyl-caged glutamate. The intracellular solution contained 140 mM NaMES and 10 mM glutamate, and the extracellular solution contained 140 mM NaMES ($V_m = 0$ mV). The *solid line* is a fit with a sum of three exponential terms (time constants for the decaying phases stated; the third phase represents the rising phase, which is most likely related to glutamate binding). *B*, similar experiment with EAAC1$_{WT}$, 1 mM 4-methoxy-7-nitroindolinyl-caged glutamate under conditions that match the fractional occupation of the glutamate binding site to that of EAAC1$_{T101A}$ in *A*.

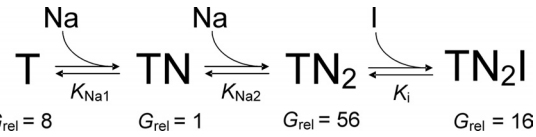

FIGURE 8. **Simplified model for the sequence of Na^+ and inhibitor binding to EAAC1$_{T101A}$.** G_{rel} denotes the conductance values for the SCN^- conductance of each state relative to the TN state, which was arbitrarily set to 1.

data (Fig. 8), the anion conductance is modulated as the transporter occupies the several states included in the model, in agreement with previous suggestions (36, 47). The state with only one Na^+ ion bound has the lowest anion conductance, whereas full activation of the Na^+-dependent anion conductance requires binding of two Na^+ ions. According to the data shown in Fig. 1, the Na^+-free state must also have residual anion conductance, because binding of one Na^+ ion inhibits tonic anion flux-mediated inward current. Thus, it appears that Na^+ binding is not absolutely required for the activation of anion conductance, in contrast to a previous proposal (18), but that Na^+ binding strongly enhances the anion conductance intrinsic to the transporter.

The T101A Mutation Does Not Eliminate Substrate Transport—Transport current recordings, as well as analysis of aspartate uptake, demonstrate that EAAC1$_{T101A}$ is able to transport glutamate across the cell membrane (Figs. 3 and 6*A*), although the transport rate is significantly lower than that of the wild type transporter. Analysis of pre-steady-state and steady-state currents suggests that the reduction of the transport rate is caused by both a 3-fold slowing of the Na^+-dependent glutamate translocation reaction and inhibition of the K^+-dependent relocation process (Fig. 6). For technical reasons we could not determine the affinity of the mutant transporter for potassium. It remains therefore an open question whether Thr^{101} participates in an overlapping sodium and potassium binding site as has been suggested for the putative Na1 binding site (28). The impact of the T101A mutation is more subtle than that of the D367N mutation, which completely eliminates glutamate transport and dramatically slows translocation (24). Why do the T101A and D367N mutations impair the binding of Na^+ to the glutamate-free form of the transporter but have differential effects on glutamate uptake? We propose that negative charge on the side chain of Asp^{367} and also on other acidic amino acid residues located in the transmembrane domain is absolutely necessary for the full function of EAAC1. Thus, charge-altering mutations, such as D367N, dramatically alter transporter properties. In contrast, the T101A mutation is not expected to result in a substantially different charge distribution in the transmembrane domains, suggesting that the lack of electrostatic effects results in a more subtle phenotype.

Does the Side Chain of Thr[101] Contribute to a Cation Binding Site?—Although indirect effects of the T101A mutation on Na^+ binding cannot *per se* be excluded, mounting evidence points to the existence of a cation binding site constituted by the side chain oxygens of Asp^{367} and Thr^{101} and possibly other ligands (main chain or side chain oxygens) that have not yet been identified. In the crystal structure of GltPh, the analogous Asp^{312} and Thr^{92} side chains both point toward a hydrophilic pocket. To test whether this pocket has the potential to harbor a cation binding site, we performed a valence screening analysis (40) of the GltPh structure, using the empirical parameters described in Equation 1 for Na^+ and K^+. Interestingly, we found a point of suitable but not optimal valence for K^+ (1.17) in a position that is surrounded by the side chains of Thr^{92}, Asp^{312}, and Asn^{310} (Fig. 9*A*), as indicated by the *arrow* and the *colored dots* overlaid on the GltPh structure. The Gly^{404} main chain carbonyl oxygen, as well as the Tyr^{88} side chain oxygen, also contribute to electrostatic compensation of the positive charge of the cation. The distances of the ligand atoms to the center of this potential cation binding site are listed in Fig. 9*B*. These distances are in the range expected for an average K^+-O pair of 2.8 Å (41). The valence for Na^+ at the same position was 0.59. This analysis suggests that this could be a potential cation binding site. However, the site does not have an optimal valence for either Na^+ or K^+, consistent with the lack of effect of K^+ on GltPh-dependent aspartate transport (23), as well as the lack of previous identification of this site through crystallography. Why does the valence screening procedure yield valences that deviate from unity for sodium? A number of possibilities have to be considered in isolation or in combination to explain this effect: 1) GltPh binds only two Na^+ ions, whereas EAAC1 binds three. If this is the case, subtle differences in geometry between the GltPh and EAAC1 structures at this site, leading to a closer spacing of the ligands to the center of the site, may result in a more optimal Na^+ valence for EAAC1. 2) The cation binding

A

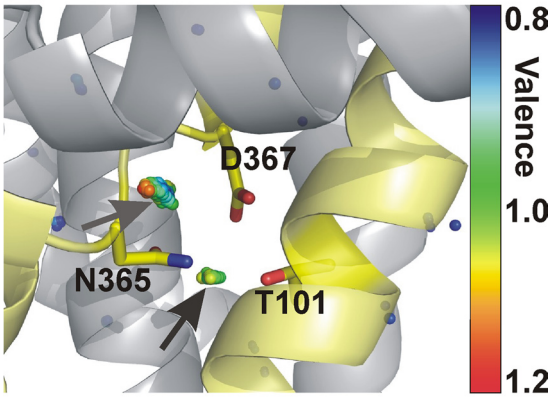

B

Oxygen atom (GltPh)	Distance from cation (Å)
D312 (side chain 1)	2.52
D312 (side chain 2)	3.65
T92 (side chain)	2.7
N310 (side chain)	2.55
G404 (backbone)	2.8
Y88 (side chain)	3.2

FIGURE 9. **Valence mapping of the GltPh structure predicts a potential cation binding site with the side chains of Asp[367] and Thr[101] as ligands.** *A*, valence map for K^+ (*colored dots*) in overlay with the GltPh structure. The *dots* illustrate points in three-dimensional space that were mapped to a valence of 0.8 (*blue*) to 1.2 (*red*) (the valence color code is shown on the *right side* of the figure). An optimal valence of 1 is color-coded *green*. Thus, *green dots* indicate a suitable binding site for K^+, as indicated by the *arrows*. Residues Thr[92], Asn[310], and Asp[312] of GltPh (Thr[101], Asn[365], and Asp[367] in EAAC1) are highlighted as *sticks*. *B*, distances of the coordinating oxygen atom to the center of the cation used for valence calculation.

site has a low affinity for cations, consistent with the experimental results showing an apparent K_m of 100 mM. 3) A Na^+ ligand in form of an additional water molecule is missing in the crystal structure, because of the limited resolution. This ligand would contribute additional electrostatic compensation, increasing the valence for sodium. The last possibility is supported by recent results from molecular dynamics simulations (48).

A third cation binding site has also been proposed by Holley and Kavanaugh (27). This site is in the proximity of the substrate binding site. Our mutagenesis data do not allow insight into this other potential cation binding site. While this work was in preparation, a molecular dynamics study suggested a third sodium binding site in the exact same location as the one proposed here (48).

REFERENCES

1. Kanai, Y., and Hediger, M. A. (2003) *Eur. J. Pharmacol.* **479,** 237–247
2. Bergles, D. E., Diamond, J. S., and Jahr, C. E. (1999) *Curr. Opin. Neurobiol.* **9,** 293–298
3. Arriza, J. L., Eliasof, S., Kavanaugh, M. P., and Amara, S. G. (1997) *Proc. Natl. Acad. Sci. U.S.A.* **94,** 4155–4160
4. Fairman, W. A., Vandenberg, R. J., Arriza, J. L., Kavanaugh, M. P., and Amara, S. G. (1995) *Nature* **375,** 599–603
5. Kanai, Y., and Hediger, M. A. (1992) *Nature* **360,** 467–471
6. Pines, G., Danbolt, N. C., Bjørås, M., Zhang, Y., Bendahan, A., Eide, L., Koepsell, H., Storm-Mathisen, J., Seeberg, E., and Kanner, B. I. (1992) *Nature* **360,** 464–467
7. Storck, T., Schulte, S., Hofmann, K., and Stoffel, W. (1992) *Proc. Natl. Acad. Sci. U.S.A.* **89,** 10955–10959
8. Levy, L. M., Warr, O., and Attwell, D. (1998) *J. Neurosci.* **18,** 9620–9628
9. Zerangue, N., and Kavanaugh, M. P. (1996) *Nature* **383,** 634–637
10. Kanner, B. I., and Sharon, I. (1978) *Biochemistry* **17,** 3949–3953
11. Wadiche, J. I., Arriza, J. L., Amara, S. G., and Kavanaugh, M. P. (1995) *Neuron* **14,** 1019–1027
12. Kanner, B. I., and Sharon, I. (1978) *FEBS Lett.* **94,** 245–248
13. Kanner, B. I., and Bendahan, A. (1982) *Biochemistry* **21,** 6327–6330
14. Kavanaugh, M. P., Bendahan, A., Zerangue, N., Zhang, Y., and Kanner, B. I. (1997) *J. Biol. Chem.* **272,** 1703–1708
15. Pines, G., and Kanner, B. I. (1990) *Biochemistry* **29,** 11209–11214
16. Otis, T. S., and Jahr, C. E. (1998) *J. Neurosci.* **18,** 7099–7110
17. Wadiche, J. I., and Kavanaugh, M. P. (1998) *J. Neurosci.* **18,** 7650–7661
18. Watzke, N., Bamberg, E., and Grewer, C. (2001) *J. Gen. Physiol.* **117,** 547–562
19. Watzke, N., and Grewer, C. (2001) *FEBS Lett.* **503,** 121–125
20. Grewer, C., Watzke, N., Wiessner, M., and Rauen, T. (2000) *Proc. Natl. Acad. Sci. U.S.A.* **97,** 9706–9711
21. Otis, T. S., and Kavanaugh, M. P. (2000) *J. Neurosci.* **20,** 2749–2757
22. Boudker, O., Ryan, R. M., Yernool, D., Shimamoto, K., and Gouaux, E. (2007) *Nature* **445,** 387–393
23. Ryan, R. M., Compton, E. L., and Mindell, J. A. (2009) *J. Biol. Chem.* **284,** 17540–17548
24. Tao, Z., Zhang, Z., and Grewer, C. (2006) *J. Biol. Chem.* **281,** 10263–10272
25. Gu, Y., Shrivastava, I. H., Amara, S. G., and Bahar, I. (2009) *Proc. Natl. Acad. Sci. U.S.A.* **106,** 2589–2594
26. Huang, Z., and Tajkhorshid, E. (2008) *Biophys. J.* **95,** 2292–2300
27. Holley, D. C., and Kavanaugh, M. P. (2009) *Philos. Trans. R. Soc. Lond. B. Biol. Sci.* **364,** 155–161
28. Teichman, S., Qu, S., and Kanner, B. I. (2009) *Proc. Natl. Acad. Sci. U.S.A.* **106,** 14297–14302
29. Rosental, N., Bendahan, A., and Kanner, B. I. (2006) *J. Biol. Chem.* **281,** 27905–27915
30. Tao, Z., Gameiro, A., and Grewer, C. (2008) *Biochemistry* **47,** 12923–12930
31. Kunkel, T. A., Roberts, J. D., and Zakour, R. A. (1987) *Methods Enzymol.* **154,** 367–382
32. Pines, G., Zhang, Y., and Kanner, B. I. (1995) *J. Biol. Chem.* **270,** 17093–17097
33. Keynan, S., Suh, Y. J., Kanner, B. I., and Rudnick, G. (1992) *Biochemistry* **31,** 1974–1979
34. Fuerst, T. R., Niles, E. G., Studier, F. W., and Moss, B. (1986) *Proc. Natl. Acad. Sci. U.S.A.* **83,** 8122–8126
35. Wadiche, J. I., Amara, S. G., and Kavanaugh, M. P. (1995) *Neuron* **15,** 721–728
36. Bergles, D. E., Tzingounis, A. V., and Jahr, C. E. (2002) *J. Neurosci.* **22,** 10153–10162
37. Grewer, C., Madani Mobarekeh, S. A., Watzke, N., Rauen, T., and Schaper, K. (2001) *Biochemistry* **40,** 232–240
38. Mim, C., Balani, P., Rauen, T., and Grewer, C. (2005) *J. Gen. Physiol.* **126,** 571–589
39. Canepari, M., Nelson, L., Papageorgiou, G., Corrie, J. E., and Ogden, D. (2001) *J. Neurosci. Methods* **112,** 29–42
40. Page, M. J., and Di Cera, E. (2006) *Physiol. Rev.* **86,** 1049–1092
41. Nayal, M., and Di Cera, E. (1996) *J. Mol. Biol.* **256,** 228–234
42. Yernool, D., Boudker, O., Jin, Y., and Gouaux, E. (2004) *Nature* **431,** 811–818
43. Shimamoto, K., Lebrun, B., Yasuda-Kamatani, Y., Sakaitani, M., Shigeri, Y., Yumoto, N., and Nakajima, T. (1998) *Mol. Pharmacol.* **53,** 195–201
44. Mim, C., Tao, Z., and Grewer, C. (2007) *Biochemistry* **46,** 9007–9018
45. Grewer, C., Watzke, N., Rauen, T., and Bicho, A. (2003) *J. Biol. Chem.* **278,** 2585–2592
46. Koch, H. P., Hubbard, J. M., and Larsson, H. P. (2007) *J. Biol. Chem.* **282,** 24547–24553
47. Tao, Z., and Grewer, C. (2007) *J. Gen. Physiol.* **129,** 331–344
48. Huang, Z., and Tajkhorshid, E. (2010) in *54th Annual Meeting of the Biophysical Society, February 20–24, 2010, San Francisco,* Biophysical Society, Rockville, MD
49. Borre, L., and Kanner, B. I. (2004) *J. Biol. Chem.* **279,** 2513–2519